COMPUTATIONAL INVESTIGATION OF UNGLAZED SELECTIVE COLLECTOR AND SINGLE ONE WITH PLEXIGLAS AS COVER BASED ON EXERGETIC PERFORMANCE CRITERIA

Aloyem Kaze C.V., PhD
Tchinda Rene, PhD
L2MSP, Faculty of Science, University of Dschang LISIE, University Institute of Technology FOTSO-VICTOR (Associated Lab), University of Dschang

Abstract

In this paper, performance assessment of two solar air systems is conducted through energy and exergy analysis. One is an unglazed selective absorber (C_1) and the second is a single one solar air with the polymethyl methacrylate as cover (C_2). The mean hourly values of solar irradiation and ambient temperature of Garoua region in Cameroon are used. The influence of the solar air heater duct depth and the number of transfer units on the exergy output is discussed. The main results we can draw are that at 12:30, the exergy output rate (Exu) of the first collector is almost five times the one of the second collector. The highest dimensionless exergy loss occurred in the collector with plastic cover while the lowest through unglazed collector. It has been also observed that for NTU (Number of Transfer Units) higher than 1.8, the exergy output rate increases weakly and becomes constant for NTU greater than 2.5.

Keywords: Unglazed selective absorber, plexiglas, energy analysis, exergy analysis, exergy loss

Introduction

The challenge of the people living in this world is to face a problem of energy in various forms. Today this energy seems to become a basic need for the world population. However, the kind of energy to be used is important. In fact, the fossil fuel energy is responsible for the climate change and must be avoided. One of the alternative ways to reduce the use of the fossil fuel is by to use of the solar air heater for some applications. These applications are essentially related to the supply of hot air to school buildings, agricultural and industrial drying (Wenfeng et al. 2007). Its advantages are low cost and no high pressure problems (Wazed et al. 2010). However, before using this system, thermal performance need to be improved. This performance depends on the material, type of the absorber, shape, dimension and layout of the collectors (Akpinar et al. 2010). It is reported in literature that heat transfer rate can be enhanced by increasing the surface area by using corrugated surfaces (Wenfeng et al. 2007, Liu et al. 2007) or extended surfaces called fins (Ho et al. 2002, Naphon 2005). Another method is to increase convective heat transfer coefficient by creating turbulence at the heat transfer surface

Nomenclature.

A_c: area element (m^2)
C_p: specific heat (J/kg.K)
d_h: equivalent diameter of air channel
E_x : exergy (w)
E_{xu}: exergy output rate ignoring pressure drop (w)
$E_{Xu,p}$: exergy output rate considering pressure drop (w)
$\dot{E}_{xdest}$ rate of irreversibility (w)
F': collector efficiency factor
f: friction factor
G: mass flow rate per unit area (kg/m^2.s)
h: heat transfer coefficient(W/ m^2K)
H or e_f solar heater duct depth (m)
I_T: radiation intensity (w/m^2)
k: thermal conductivity (W/mK)
$\dot{m}$: mass flow rate (kg/h)
Nu: Nusselt number
NTU: Number of transfer units
P: pressure (N/m^2)
Pr: Prandtl number
Re: Reynolds number
s : entropy (J/kg .k)
S: incident solar radiation (w/m^2)
T: temperature (K)
t: time (h)
U: loss coefficient (W/ m^2K)
V: wind speed (m/s)
SAH: Solar air heaters
W_p: pump work (w)
x,y: space coordinate

Greek letters

□ : solar absorbance
δ : thickness (m)
ε : emissivity
σ : Stefan-Boltzmann constant
t: Transmitivity
ρ : reflectance
ρf : fluid density (kg/m^3)
Δp : pressure drop (N/m^2)
η_{pm} : pump-motor efficiency
ψ_s : Exergy efficiency of radiation

Subscript:

a: ambient
b: bottom plate
c: convection, cover
f: fluid (air)
fi : inlet
fo: outlet
p: absorber plate
r: radiation
s: selective
t: top

by providing artificial roughness on underside of the absorber plate (Karwa et al. 2001, Layek et al. 2007, Saini et al. 2008). Finally, investigations also showed that heat transfer can be improved by using the selective coatings on the absorber of conventional solar air heater (El-Sebai et al. 2010) or simply an unglazed selective absorber (USA) (Njomo et al. 2006). Tchinda (2009) published recently a review on the mathematical models performed for predicting thermal performance of solar air systems. He noticed that the major governing equation in the models were investigated using the first law of thermodynamic.

In that way, Njomo et al. (2006) made the theoretical study of an USA and the solar air heater with Plexiglas as cover considering operating conditions of the Garoua town.

An unglazed selective absorber is a renewable energy technology with a considerable potential for commercial and industrial applications. Some applications such as sun drying in agricultural sector and paring photovoltaic and thermal systems with USA are regularly considered (Chow et al. 2010). Researches also showed that the cost of solar air heaters is significantly reduced when using bare collectors with selective porous or non-porous absorbers (Verma et al. 1991, Kutscher et al. 1994). On the other hand, with the purpose to collect maximum energy at the minimum cost, the glass usually used in solar air heater as cover can be replaced by the plastic like the polymethyl methacrylate (plexiglas)(Njomo, 1995) . Due to the importance and the applications of these collectors in thermal process as mentioned above, it becomes important to pay more attention on them. Previous work (Njomo et al. 2006) did not take into account the pressure drop in the duct of collectors and the energy analysis alone can not be a criterion for the optimization of the systems. Therefore, in order to take into consideration those insufficiencies, the theory of exergy is used for evaluating performance and optimizing the designed heater.

The first law of thermodynamics deals with the quantity of energy and insists on the fact that energy can not be created or destroyed while the second law deals with the quality of energy. To balance the quantity and the quality of heat transfer during thermal process, exergy analysis is suitable. It is important to use the concept of exergy balance in the analysis of thermal systems. That exergy balance is a statement of the law of degradation of energy due to the irreversibilities of all real processes. The exergy of a system can be defined as the maximum useful work possible during a process that brings the system into equilibrium with the environment. An exergy analysis is a powerful mathematical tool in the design, assessment, optimization and improvement of complex thermodynamic systems. Many authors (Bejan et al. 1981, Bejan 1986, Gupta et al. 2008) published papers in connexion with the governing equations of exergy balance to be applied to solar collectors. From those works, the popularity of exergy analysis method has considerably grown.

The main purpose of this paper is to go beyond the above restrictive assumption concerning the pressure drop and energy analysis. In this study, the energy and exergy analyses is done to investigate the performance of an unglazed selective absorber (collector C_1) and the collector with Plexiglas as cover (collector C_2) when functioning in the same operating conditions and with the same dimensions. The influence of daily means hourly values of solar irradiation in May at Garoua ($9^o20^’$ N; $13^o23^’$ E), the solar air heater duct depth and the Number of transfer units on the exergy output is discussed among others.

Thermodynamic modelling:

An USA collector is a bare collector with the selective absorber and made of an absorber plate whose irradiated surface is covered with a selective coating that has the radiation properties $\alpha_s = 0.92$ and $\varepsilon_s = 0.13$ (Njomo et al. 2006). The shaded surface of this plate ($\alpha_p = \varepsilon_p = 0.8$) and the back metallic plate are painted with black colour.

After neglecting the time rates of change of the enthalpies of the different components of the collectors and under steady state, one can write the following energy balance equations based on the first law of thermodynamic as

For the collector C_1 (Fig. 1)

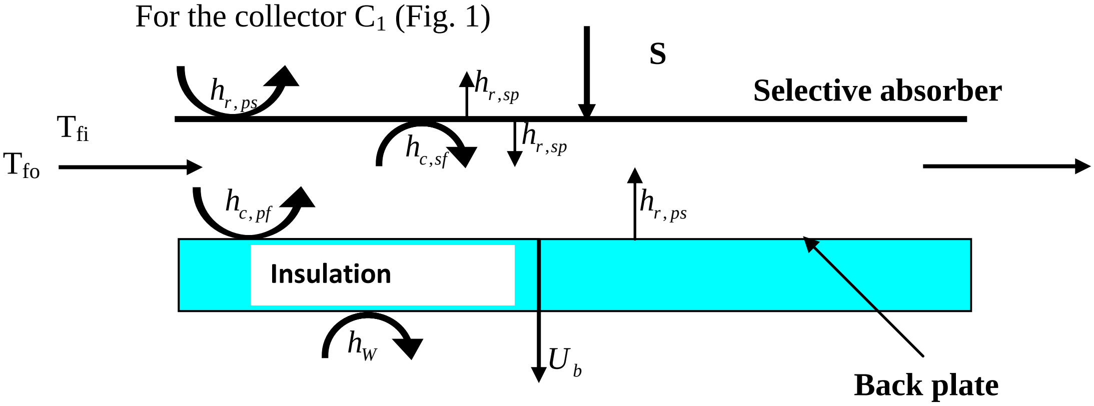

Fig.1. Unglazed selective absorber (USA)

- **For selective absorber**

$$\alpha_s I_T = h_{r,ps}\left(T_s - T_p\right) + h_{c,sf}\left(T_s - T_f\right) + \left(h_{c,sa} + h_{r,sa}\right)\left(T_s - T_a\right)$$

(1)

- **For back plate**

$$h_{r,ps}\left(T_s - T_p\right) = h_{c,pf}\left(T_p - T_f\right) + U_b\left(T_p - T_a\right)$$

(2)

Energy balance equations for collector C_2 (Fig.2)

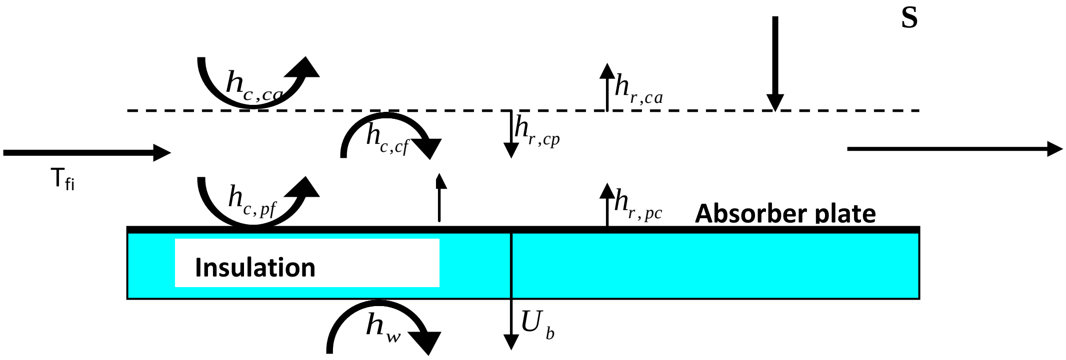

Fig. 2. Single cover solar air heater with the Plexiglas as the cover

- **For the transparent cover**

$$\alpha_c I_T = h_{r,pc}\left(T_p - T_c\right) + h_{c,cf}\left(T_f - T_c\right) + \left(h_{c,ca} + h_{r,ca}\right)\left(T_c - T_a\right)$$
(3)

- **For the absorbing plate**

$$(1.01\tau_c\alpha_p)I_T = \left(U_b + h_{r,pa}\right)\left(T_p - T_a\right) + h_{c,pf}\left(T_p - T_f\right) + h_{r,pc}\left(T_p - T_c\right)$$
(4)

For the air flowing through the channel of collectors, one can write

$$\rho H c_{pf}\frac{\partial T_f}{\partial t} = h_{c,jf}\left(T_j - T_f\right) + h_{c,pf}\left(T_p - T_f\right) - \frac{\dot{m}c_p}{\ell}\frac{\partial T_f}{\partial x},\ j = c, s$$
(5)

Solving Eqs.(1), (2), (3) and (4) for T_p and T_j considering the following boundary condition

$$T_f\big|_{x=0} = T_{fin}$$
(6)

The outlet temperature for collector C_1 can be written from Eq.(5) as:

$$T_{fo} = -\frac{c_{1s} + c_{1p} + (c_{3s} + c_{3p})T_a}{c_{2s} + c_{2p} - 2} + \left[T_{fin} + \frac{c_{1s} + c_{1p} + (c_{3s} + c_{3p})T_a}{c_{2s} + c_{2p} - 2}\right]\exp\left(\frac{b}{c_p G}\right)$$

(7)

where

$$h_{Ts} = h_{r,ps} + h_{c,sf} + h_{c,sa} + h_{r,sa}$$

(8)

$$h_{Tp} = h_{r,ps}\left(1 - \frac{h_{r,ps}}{h_{Ts}}\right) + h_{c,pf} + U_b$$

(9)

$$h_{Ta} = h_{c,sa} + h_{r,sa}$$

(10)

$$h_{Tf} = \frac{h_{c,sf} h_{r,ps}}{h_{Ts}} + h_{c,pf}$$

(11)

$$h_{Ta1} = \left(h_{r,ps} + U_b\right)\frac{h_{Ta}}{h_{Ts}}$$

(12)

$$c_{1p} = \frac{\left(\alpha_s I_T\right) h_{r,ps}}{h_{Tp} h_{Ts}}$$

(13)

$$c_{2p} = \frac{h_{Tf}}{h_{Tp}}$$

(14)

$$c_{3p} = \frac{h_{Ta1}}{h_{Tp}}$$

(15)

$$c_{1s} = \frac{\alpha_s I}{h_{Ts}}\left(1 - \frac{h_{r,ps}^2}{h_{Tp} h_{Ts}}\right)$$

(16)

$$c_{2s} = \frac{h_{c,sf}}{h_{Ts}} + \frac{h_{Tf} h_{r,ps}}{h_{Tp} h_{Ts}}$$

(17)

$$c_{3s} = \frac{h_{Ta}}{h_{Ts}} + \frac{h_{Ta1} h_{r,ps}}{h_{Tp} h_{Ts}}$$

(18)

$$b = h_{c,pf}\left(-2 + \frac{h_{c,sf}}{h_{Ts}} + \frac{h_{Tf}}{h_{Tp}} + \frac{h_{Tf} h_{r,ps}}{h_{Tp} h_{Ts}}\right)$$

(19)

and for the second collector

$$T_{f0} = -\frac{\left[\left(c_4 + ac_{12}\right) + \left(c_2 + ac_{14}\right)T_a\right]}{-2 + c_1 + ac_{13}} + \left(T_{fin} + \frac{\left[\left(c_4 + ac_{12}\right) + \left(c_2 + ac_{14}\right)T_a\right]}{-2 + c_1 + ac_{13}}\right)\exp\left(\frac{b_o}{Gc_p}\right)$$

(20)

where

$$h_{Tc} = h_{r,pc} + h_{c,cf} + h_{c,ca} + h_{r,ca}$$

(21)

$$h_{Ta} = h_{c,ca} + h_{r,ca}$$

(22)

$$h_{Tp} = U_b + h_{r,p_a} + h_{c,pf} + h_{r,pc}$$

(23)

$$h_{Ua} = U_b + h_{r,pa}$$

(24)

$$c_1 = \frac{h_{c,pf} + h_{r,pc}}{h_{Tp} - \frac{h_{r,pc}^2}{h_{Tc}}}$$

(25)

$$c_2 = \frac{h_{Ua}h_{Tc} + h_{r,pc}h_{Ta}}{h_{Tp}h_{Tc} - h_{r,pc}^2}$$

(26)

$$c_4 = \frac{h_{Tc}}{h_{Tp}h_{Tc} - h_{r,pc}^2}\left[\left(\alpha\tau\right)I_T + \alpha_c I_T\left(\frac{h_{r,pc}}{h_{Tc}}\right)\right]$$

(27)

$$ac_{12} = \frac{\alpha_c I_T}{h_{Tc}} + \frac{h_{r,pc}}{h_{Tp}h_{Tc} - h_{r,pc}^2}\left[\left(\alpha\tau\right)I_T + \alpha_c I_T\left(\frac{h_{r,pc}}{h_{Tc}}\right)\right]$$

(28)

$$ac_{13} = \frac{h_{r,pc}\left(h_{c,pf} + h_{r,pc}\right)}{h_{Tp}h_{Tc} - h_{r,pc}^2} + \frac{h_{c,pf}}{h_{Tc}}$$

(29)

$$ac_{14} = \frac{h_{Ta}}{h_{Tc}} + \frac{h_{r,pc}}{h_{Tc}}\left(\frac{h_{r,pc}h_{Ta} + h_{Tc}\left(U_b + h_{r,pa}\right)}{h_{Tp}h_{Tc} - h_{r,pc}^2}\right)$$

(30)

$$b_o = h_{c,pf}\left[-2+\frac{h_{Tc}\left(h_{c,pf}+h_{r,pc}\right)}{h_{Tp}h_{Tc}-h_{r,pc}^2}+\frac{h_{r,pc}\left(h_{c,pf}+h_{r,pc}\right)}{h_{Tp}h_{Tc}-h_{r,pc}^2}+\frac{h_{c,pf}}{h_{Tc}}\right]$$

(31)

Hydraulic performance:

Hydraulic performance of a solar air heater concerns pressure drop (Δp) in the duct. Pressure drop accounts for energy consumption by fan to propel air through the duct. It can be presented in non-dimensional form by using the following relationship of friction factor (f) reported by Franck et al. (2001).

$$f = \frac{\Delta p d_h}{2\rho L_1 V^2}$$

(32)

Where the characteristic dimension or equivalent diameter of **SAH** duct is given by:

$$d_h = \frac{2lH}{\left(l+H\right)}$$

(33)

The Reynolds Number Re is calculated by :

$$\mathrm{Re} = \frac{\rho V d_h}{\mu}$$

(34)

For the laminar flow, $\mathrm{Re} \le 2300$, and the coefficient of friction f is calculated by :

$$f = 16/\mathrm{Re}$$

(35)

Otherwise the coefficient of friction for the turbulent flow in **SAH** is calculated from Blasius equation which is :

$$f = 0.079(\mathrm{Re})^{-\frac{1}{4}}$$

(36)

The pump work w_p is defined as follow :

$$W_p = \dot{m}\Delta p \Big/ (\eta_{pm}\rho)$$

(37)

Energy and exergy analysis:

The following assumption have been made in this study

(i) Steady state, steady flow operation

(ii) Negligible potential and kinetic energy effects and no chemical and nuclear reaction

(iii) Air is and ideal gas with a constant specific heat and its humidity content is ignored.

Exergy is defined as the maximum amount of work which can be produced by a system. For real processes, there are still a difference between the exergy input and the exergy output due to irreversibilities.

The exergy flows in the collectors are illustrated in the following Figure 3.

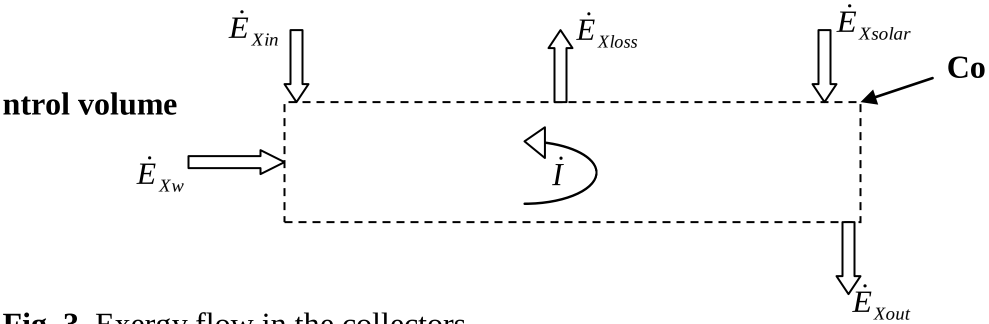

Fig .3. Exergy flow in the collectors

An exergy balance for collectors C_1 and C_2 can be writing as:

$$\dot{E}_{Xsolar} + \dot{E}_{Xw} + \dot{E}_{Xin} = \dot{E}_{Xloss} + \dot{E}_{Xout} + \dot{E}_{Xdest}$$
(38)

The exergy destruction or the irreversibility may be expressed as follow (Ucar et al. 2006)

$$\dot{I} = \dot{E}_{Xdest} = T_a \dot{S}_{gen}$$
(39)

Due to the fact that the process is irreversible, the exergy destruction is $\dot{I}$ is greater than zero.

$$\dot{E}_{Xin} = \dot{m}\left[\left(h_{in} - h_a\right) - T_a\left(s_{in} - s_a\right)\right]$$
(40)

$$\dot{E}_{Xout} = \dot{m}\left[\left(h_{out} - h_a\right) - T_a\left(s_{out} - s_a\right)\right]$$
(41)

The Petela (2008) expression for the available energy flux is used to calculate the exergy of solar radiation.

$$\dot{E}_{Xsolar} = I_T A_C \left[1 - \frac{4T_a}{3T_S} + \frac{1}{3}\left(\frac{T_a}{T_S}\right)^4 \right]$$

(42)

For other components, the following relationships are available

$$\dot{E}_{Xw} = \frac{\dot{m}\Delta p}{\rho}$$

(43)

$$\dot{E}^{j}_{Xloss} = \left(q^{j}_{c-loss} + q^{j}_{r-loss}\right)\left(1 - \frac{T_a}{T_j}\right) \qquad j = s, c$$

(44)

Where

$$q^{j}_{c-loss} = \frac{Nuk_a A_c}{H}\left(T_j - T_a\right)$$

(45)

$$q^{j}_{r-loss} = \varepsilon_j \sigma A_C \left(T_j^4 - T_{sky}^4\right)$$

(46)

The useful exergy or exergy output rate "E_{xu}" can be expressed as

$$E_{xu} = \dot{m}\left[\left(h_{ou} - h_{in}\right) - T_e\left(s_{ou} - s_{in}\right)\right]$$

(47)

The actual exergy rate $E_{xu,p}$ delivered considering pressure drop of collector fluid is (Gupta et al. 2009)

$$E_{xu,p} = E_{xu} - E_{xdp}$$

(48)

where

$$E_{xdp} = \frac{T_e}{T_i} W_p$$

(49)

and Eq.(48) becomes

$$E_{xu,p} = \dot{m}\left[\left(h_{ou} - h_{in}\right) - T_e\left(s_{ou} - s_{in}\right)\right] - \frac{T_e}{T_i}$$

(50)

According to Kurbas et al. (2004) , the dimensionless exergy loss by the system can be defined as

$$E = \frac{\dot{E}_{xu}}{Q}, \quad Q = \dot{m} c_p \left(T_{fo} - T_{fi}\right)$$

(51)

Based on the first law of thermodynamics, the thermal efficiency of solar air heater is defined as:

$$\eta_I = \frac{Qu}{A_c I_T}$$

(52)

The daily thermal energy efficiency is defined by the following expression

$$\eta_{I_{daily}} = \frac{\int_{6am}^{6pm} \dot{m} c_p \left(T_{f_0} - T_{fin}\right) dt}{A_c \int_{6am}^{6pm} I_T dt}$$

(52)

The exergy collection efficiency (η_{II}) based on the second law of thermodynamics is defined as the ratio of useful exergy $E_{xu,p}$ to the exergy of incident solar radiation.

$$\eta_{II} = \frac{E_{xu,p}}{A_c I_T \psi_s}$$

(53)

Exergy output rate and number of transfer units:

Taking into account the fact that $h_{c,cf} = h_{c,sf} = h_{c,pf} = h$ (Njomo et al. 2006) for the two collectors, the energy balance of the air flow of the two collectors can be rewritten as:

$$\frac{\dot{m} c_p}{l} \frac{dT_f}{dx} = h\left(T_i + T_j - 2T_f\right)$$

(54)

Where T_i and T_j are the temperature of the matter which is above and below the fluid flowing through the duct respectively.

The number of transfer units of the fluid is given by (Kurbas et al. 2007):

$$NTU = \frac{\text{heat capacity of heat exchange}}{\text{heat capacity of flow}}$$

(55)

Setting

$$X = \frac{x}{L}$$

(56)

Eq. (54) becomes

$$\frac{dT_f}{dX} = N\left(T_i + T_j - 2T_f\right)$$

(57)

Solving Eq.(57) with the following boundary conditions:

At $X = 0, \mathrm{T_f} = T_{fin}$ and at X=1 , $\mathrm{T_f} = T_{fo}$, one gets ,

(58)

$$T_{fo} = \frac{1}{2}\left[\left(T_i + T_j\right) - \left(T_i + T_j - 2T_{fin}\right)\exp\left(-2N\right)\right]$$

(59)

$$\text{Take } \theta = \frac{T_i + T_j}{T_{fi}}$$

(60)

Eq .(50) becomes

[illegible]

(61)

The daily exergy output rate for some value of Number of transfer units is obtained by integrating the expression (61) from 6 a.m to 6 p.m.

Evaluation of the heat transfer coefficients:

For the collectors C_1-C_2, the wind transfer coefficient $h_{c,ja}$ over the selective absorber and the transparent cover is calculated using the relationship

$$h_{c,ja} = \frac{N_u^{'} k_a}{L_s}$$

(62)

In the above equation, the Nusselt number $N_u^{'}$ is given for rectangular plates as Sparrow et al. [26]

$$N_u^{'} = 0.86\,\mathrm{Re}^{'1/2}\,\mathrm{Pr}^{1/3}$$

(63)

Where

$$\mathrm{Re}^{'} = \frac{V_a L_s}{\nu_a}$$

(64)

The Reynolds number cover the range

$$2\times10^4 < \mathrm{Re}^{'} < 9\times10^4$$

(65)

The following equation gives the convective heat transfer coefficient $h_{c,sf}$ and $h_{c,pf}$ between the hot fluid and the walls of the air channel:

$$h_{c,pf} = h_{c,sf} = \frac{Nuk_a}{d_h}$$

(66)

To evaluate the Nusselt number, the following correlations for air, for fully developed turbulent flow (if length to equivalent diameter ratio exceeds 30) with one side heated and the other side insulated is appropriate:

$$Nu = \frac{h_{c,pf} d_h}{k_a} = 0.0158\left(\mathrm{Re}\right)^{0.8}$$

(67)

If the flow is laminar then following correlation by Mercer from Duffie et al. (1980) for the case of parallel smooth plates with constant temperature on one plate and other plate insulated is appropriate:

$$Nu = \frac{h_{c,pf} d_h}{k_a} = 4.9 + \frac{0.0606\left(\mathrm{Re}\times pr\,\dfrac{d_h}{L_1}\right)^{0.5}}{1+0.0909\left(\mathrm{Re}\times pr\,\dfrac{d_h}{L_1}\right)^{0.7}\left(pr\right)^{0.17}}$$

(68)

The Reynolds number here is given by

$$\mathrm{Re} = \frac{\dot{m} d_h}{\ell H \mu_f}$$

(69)

The radiative heat transfer coefficient $h_{r,sa}$ and $h_{r,ca}$ between the selective absorber and the transparent cover and the sky are given by (Duffie et al. 1980, Njomo 2000):

$$h_{r,ja} = \frac{\varepsilon_j \sigma \left(T_j^4 - T_{sky}^4\right)}{T_j - T_a}$$
(70)

The sky temperature used in this work is:

$$T_{sky} = T_a - 6$$
(71)

The radiative heat transfer coefficient $h_{r,ps}$ between the selective absorber and the back plate both consider as parallel plates is calculated as follow (Njomo 2000):

$$h_{r,ps} = \varepsilon_{pp} \sigma \left(T_s^2 + T_p^2\right)\left(T_s - T_p\right)$$
(72)

where

$$\varepsilon_{pp} = \frac{2}{\varepsilon_p} - 1$$

The radiation heat transfer coefficients, $h_{r,pc}$ between absorber plate and plastic cover, and $h_{r,pa}$ between absorber and sky, are evaluated by taking into account that the cover is partially transparent to IR radiation; therefore one can write (Njomo et al. 2006):

$$h_{r,pc} = \frac{\varepsilon_p \sigma \left[T_p^4 \left(1 - \rho_c\right) - \varepsilon_c T_c^4\right]}{\left(1 - \rho_p \rho_c\right)\left(T_p - T_c\right)}$$
(73)

and

$$h_{r,pa} = \frac{\tau_{ir} \varepsilon_p \sigma \left(T_p^4 - T_{sky}^4\right)}{T_p - T_a}$$
(74)

The effective product transmittance-absorptance $(\tau\alpha)$ of collector C_2 can be evaluated by using the following equation:

$$(\tau\alpha) = \frac{\tau_c \varepsilon_p}{1 - (1 - \varepsilon_p)\rho_c} = 1 - \tau_c$$
(75)

Numerical simulations:

In order to evaluate the daily exergy efficiency for some values of mass flow rate per unit area of the collector (G), the daily energy output rate and the daily exergy output rate for some value of Number of transfer units

(NTU), numerical calculations have been carried out for a collector configuration, system properties and operating conditions. The means hourly values of global solar radiation and ambient air temperature in May at Garoua (9°20' N; 13°23' E) in Cameroon are used.

Since radiation heat coefficients and convective heat transfer coefficients between the flowing hot fluid and channel walls are non-linear functions of the temperatures of the collector and the mass flow rate respectively, to overcome this issue, first initial values of T_c, T_p, T_s are assumed according to inlet temperature of air and various heat transfer coefficients are calculated; and new values of those temperatures are calculated. If the calculated new values temperatures are different than the previously assumed values then the iteration is repeated with these new values till the absolute differences of new value and previous value of temperatures are less than or equal to 0.001. The temperature difference is calculated using Eqs.(17)-(19). The daily exergy output rate for some values of Number of transfer units (NTU) is performed using Eq.(61) and the exergy output is obtained from Eq.(50). In order to obtain the results numerically, codes are developed in Matlab-7.0 .

Results and discussion:

The Fig.4 presents the variations of temperature difference with incident radiation for collector C_1 and C_2. This plot of temperature versus insulation gives us an opportunity to estimate the fluid temperature for any time of the day with the help of available meteorological data of the Garoua region. The highest difference temperature (33.06°K) occurs in the first collector at 12:30 for G=0.02kg/m^2.s, H=2cm and Tfi=Ta. At the same time, we found a difference temperature of 21.36°K in the second collector considering the same operating conditions.

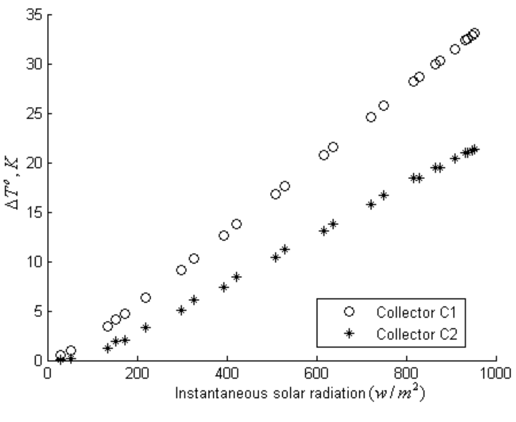

Fig. 4: Variation of instantaneous solar radiation and temperature difference

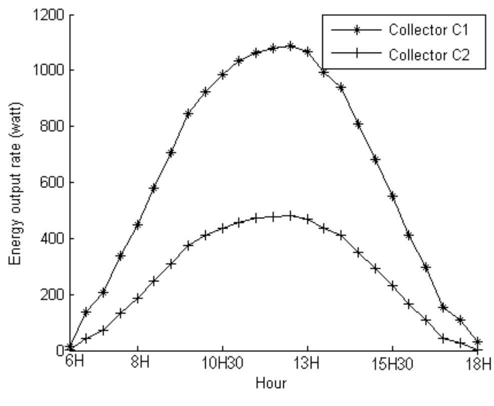

Fig. 5: Variation of the daily energy output rate with time

The Fig.5 presents the variations of the energy output rate with time along the whole day. The maximum energy output rate for collector C_1 and collector C_2 are determined as 1086.10 w and 480.17 w respectively. The Fig. 6 presents the effect of the mass flow rate on the energy efficiency for the two collectors. We observe that the energy efficiency of the collectors increases with increasing mass flow rate G. This can be explained by the rapid enhancement of the internal thermal convective exchanges in the collectors added to the slight variation of the overall thermal losses. In general the collector C_1 (USA) presents the best heat performance on the collector C_2. The influence of the mass flow per unit area G on the exergy collection efficiency based on the second law of thermodynamics is presented in Fig .7.

This figure shows that the exergy efficiency doesn't increases monotonically with G. In fact, for low inlet temperature the exergy efficiency first increases and reaches its maximum value and then after that it decreases with mass flow rate in the laminar flow regime (Re<2300); the exergy collection efficiency also decreases in the turbulent flow regime (Re>2300).

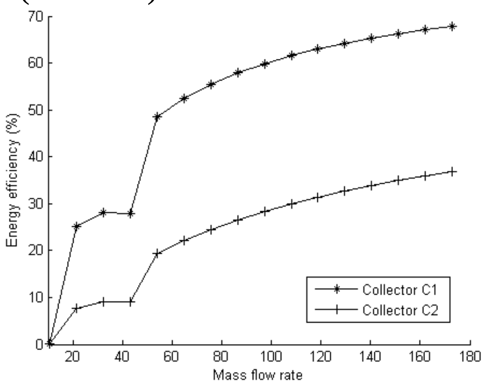

Fig. 6: Variation of the thermal energy efficiency with mass flow rate (kg/m^2.h).

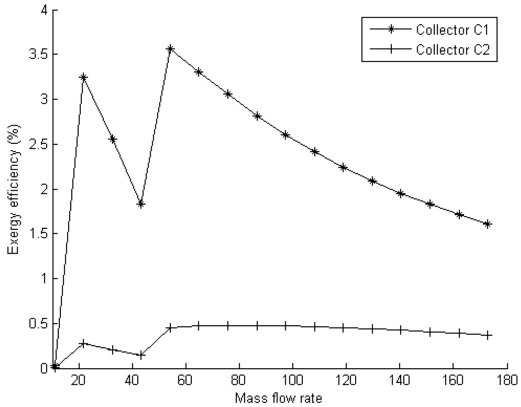

Fig.7: Variation of the exergy efficiency versus mass flow rate (kg/m^2.h)

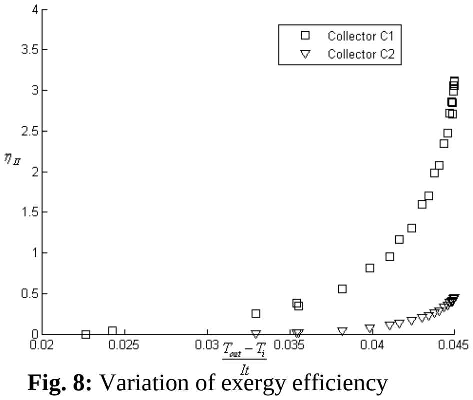

Fig. 8: Variation of exergy efficiency versus $(T_{out} - T_i)/It$

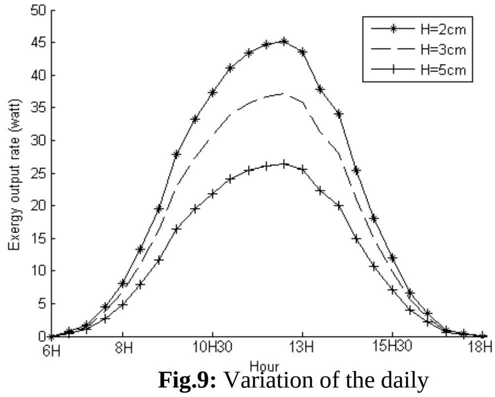

Fig.9: Variation of the daily exergy output rate for collector C1

Based on the meteorological conditions and the configuration system of the collectors, we drew in Fig.8 the variation of the exergy efficiency (η_{II}) versus $(T_{out} - T_i)/It$ for G=0.01kg/m^2.s and we observe that the η_{II} increases with $(T_{out} - T_i)/It$. The Figs. (9-10) shows the variations of the exergy output rate with time for three values of solar air heater duct depth (H=2cm; H=3cm and H=5cm). The exergy output rate of collectors C_1 and C_2 increases with the solar air heater duct depth. At the noon, the exergy output rate of the first collector is 45.12 w while the second presents the value 9.01w for H=2cm. One can notice once more that the highest Exu value is obtained by SAH with selective absorber. Figs.(11-12) presents the variations of the exergy output with the time for four values of number of

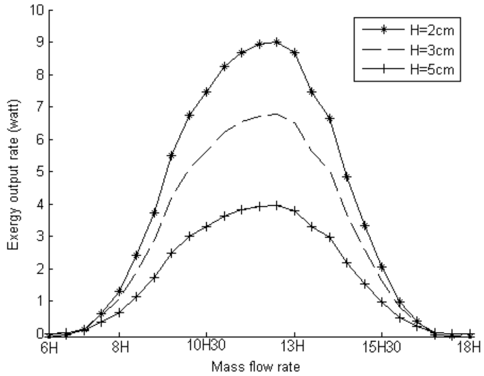

Fig.10: Variation of the daily exergy output rate for collector C2

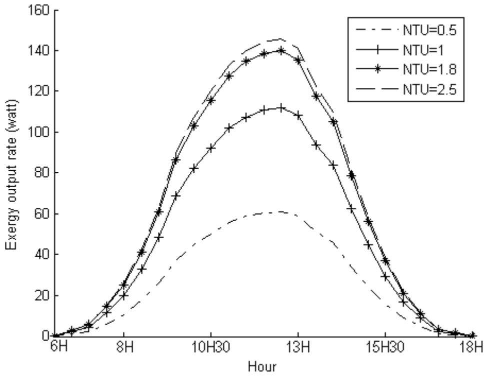

Fig.11: Variation of the daily exergy output rate for some values of NTU: Collector C1

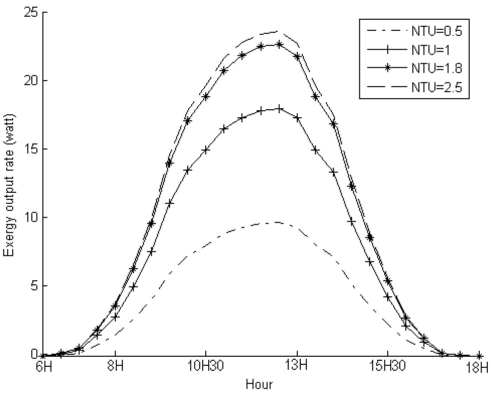

Fig12: Variation of the daily exergy output rate For some values of NTU: Collector C2

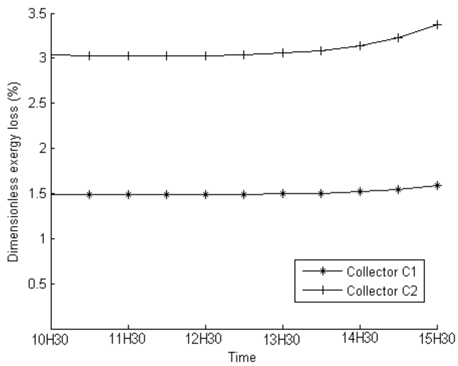

Fig.13: Variation of the dimensionless exergy loss versus time

transfer units (NTU=0.5; NTU=1; NTU=1.8; NTU=2.5). It is clear from these figures that the exergy output rate increases with the NTU for collectors C_1 and C_2. This situation can be explained by the fact that by maintaining the mass flow rate per unit area G, the collector area A_c and the specific heat constant, when the NTU increases, the convective heat transfer coefficient also increases and the consequence is the improvement of the exergy output rate. Finally, we have observed that for NTU higher than 1.8, the Exu increases weakly and becomes constant for NTU greater than 2.5. The last figure gives the representation of the dimensionless exergy loss with time between 10:30 to 15:30. It is clear from that figure the lowest exergy loss occurs in the unglazed selective absorber. At noon for example, the exergy loss through collector C_1 and C_2 is 1.48% and 3.02 % respectively for H=2cm and G=0.02kg/m^2.s.

Conclusion

Theoretical investigations of the thermal performance of the unglazed collector and the collector with Plexiglas as cover have been carried out. From the analysis, it mainly comes out that the collector C_1 presents the highest exergetic heat performance and for NTU higher than 1.8, the exergy output rate increases weakly and becomes constant for NTU greater than 2.5. In the turbulent flow regime the exergy output rate decreases when the mass flow rate per unit area increases and the highest exergy loss occurred in the collector C_2 (3.02%). A high exergy ratio between the two collectors has also been observed.

This study is important for the designed and the implementation of these systems for some heating and drying applications.

References:

Akpinar EK, Koçyigit F. (2010) Energy and exergy analysis of a new flat-plate solar air heater having different obstacles on absorber plates Appl Energy.

Bejan A, Kearney DW, Kreith F (1981). Second law Analysis and Synthesis of Solar collector Systems. Journal of Solar Energy Engineering ,103:23-28.

Bejan A. Entropy Generation Minimization. CRC Press, Boca Raton, Fla, USA, 1986

Chow TT, Pei G, Fong KF, Lin Z, Chan ALS, Ji J (2010). Energy and exergy analysis of photovoltaic-thermal collector with and without glass cover. Applied Energy, 86:310-316.

Duffie JA, Beckmann WA. Solar Engineering of thermal processes. Wiley, New York 1980.

El-Sebaii AA, Al-Snani H (2010). Effect of selective coating on the thermal performance of flat plate solar air heaters. Energy, 35:1820-1828.

Frank K, Mark SB. Principles of heat transfer. Colorado: Thomson Learning Inc; 2001.

Gupta MK, Kaushik SC (2008). Performance evaluation of solar air heater for various artificial roughness geometries based on energy, effective and exergy efficiency. Renewable Energy, 1-12.
Gupta MK, Kaushik SC (2009). Performance evaluation of solar air heater having expanded metal mesh as artificial roughness on absorber plate. Int. J. of Thermal Sciences, 48:1007-1016.
Ho MY, Chu DH, Jun ZH (2002). Collector efficiency of double flow solar air heaters with fin attached. Energy, 27: 715-727.
Karwa R, Solanki SC, Saini JS (2001). Thermo-hydraulic performance of solar air heaters having integral chamfered rib roughness on absorber plates. Energy, 26:161-176
Kutscher CF, Christensen CB, Barker GM (1994). Unglazed transpired solar collectors for dessicant cooling. Solar Energy , 52:419-427.
Kurtbas I, Durmus A (2004). Efficiency and exergy of a new solar air heater. Renewable Energy, 29:1584-1501.
Kurbas I, Durmus A, Haydar E, Turgut E (2007). Effect of propeller type swirl generators on the entropy generation and efficiency of heat exchangers. International Journal of Thermal sciences, 46:300-307.
Layek A, Saini JS, Solanki SC (2007). Second law optimization of a solar air heater having chamfered rib-groove roughness on absorber plate, Renewable Energy, 32: 1967-1980.
Liu T, Lin W, Gao W, Luo C, Li M, Zheng Q (2007). Parametric study of thermal performance of a solar air collector with a V-groove absorber. International Journal of Green Energy , 4: 427-451.
Naphon P (2005). On the performance and entropy generation of the double-pass solar air heater with longitudinal fins. Renewable Energy, 30: 1345-1357.
Njomo D (1995). Techno-economic analysis of a plastic cover solar air heater. Energy Conversion and Management, 36:1023-1029.
Njomo D (2000). Unglazed selective absorber solar air collector: heat exchange analysis.
Heat Mass Transfer, 36:313-317.
Njomo D, Daguenet M (2006). Sensitivity analysis of thermal performances of flat plate solar air heaters. Heat Mass Transfer, 42 :1065-1081.
Petela R (2008).An approach to the exergy analysis of photosynthesis. Solar Energy, 82:311–328.
Tchinda René (2009). A review of the mathematical models for predicting solar air heaters systems. Renewable and Sustainable Energy Reviews, 13:1734–1759.
Saini RP, Verma J. Heat transfer and friction factor correlations for a duct having dimple - shape artificial roughness for solar air heaters (2008). Energy, 33:1277-1287.

Sparrow EM, Ramsey JW, Mass EA. Effect of finite width on heat transfer and fluid low about an inclined rectangular plate (1979). J Heat Trans ASME ,101:199-204.
Ucar A, Inalli M (2006). Thermal and exergy analysis of solar air collectors with passive augmentation techniques. International Communication in Heat and Mass Transfer, 33:1281-1290.
Verma R, Chandra R, Garg HP (1991). Parametric studies on the corrugated solar air heaters with and without cover. Renewable Energy, 1:361-371.
Wazed MA, Nukman Y, Islam MT (2010). Design and fabrication of a cost effective solar air heater for Bangladesh. Appl Energy, doi:10. 1016/j.apenergy. 2010.02.014.
Wenfeng G, Tao L, Chaofeng X (2007). Analytical and Experimental studies on the thermal performance of cross-corrugated and flat-plat solar air heaters. Appl Energy, 84: 425-441.